JOURNAL OF AGRICULTURAL AND FOOD CHEMISTRY

Article

pubs.acs.org/JAFC

Thermodynamic and Kinetic Properties of a New Myrtillin−Vescalagin Hybrid Pigment

Ignacio García-Estévez,[†] Raquel Gavara,*[,§] Cristina Alcalde-Eon,[†] Julián C. Rivas-Gonzalo,[†] Stéphane Quideau,[#] M. Teresa Escribano-Bailón,*[,†] and Fernando Pina[§]

[†]Grupo de Investigación en Polifenoles (GIP), Facultad de Farmacia, Universidad de Salamanca, E37007 Salamanca, Spain

[§]REQUIMTE, Departamento de Química, Faculdade de Ciências e Tecnologia, Universidade Nova de Lisboa, 2829-516 Monte de Caparica, Portugal

[#]Université de Bordeaux (ISM, CNRS-UMR 5255), Institut Européen de Chimie et Biologie, 2 rue Robert Escarpit, 33607 Pessac Cedex, France

ABSTRACT: During red wine maturation in contact with oak wood, *C*-glucosidic ellagitannins can react with anthocyanins, leading to new pigments. In this work the thermodynamic and kinetic constants of the network pH-dependent equilibrium of a new myrtillin (delphinidin 3-*O*-glucoside)−vescalagin hybrid pigment (1-deoxyvescalagin-(1β→8)-myrtillin) have been determined by UV−visible absorption and stopped-flow experiments and compared to those determined for myrtillin. The vescalagin substitution at the C-8′ center of myrtillin entails important variations in the pigment behavior upon pH changes. The hybrid pigment showed lower pK'_a and pK_a values and a much higher value of K_t. As a consequence, at moderately acidic pH values ($4 < pH < 6$), the percentage of the hemiketal is much lower and the quinoidal base and the (*E*)-chalcone represent higher percentages relative to those for myrtillin. Therefore, the hybrid pigment can provide in slightly acidic or neutral solutions an exceptionally different color compared to that of myrtillin.

KEYWORDS: *anthocyanins, myrtillin (delphinidin 3-O-glucoside), ellagitannin, thermodynamic, kinetic, red wine*

INTRODUCTION

Anthocyanins are natural pigments responsible for a wide range of colors in vegetables, fruits, and derived products, such as red wines or juices.[1] In particular, they are mainly responsible for the reddish-blue color of young red wines. During aging and storage of red wine, anthocyanins are progressively transformed into new pigments responsible for important changes in the color.[2−5] These new pigments usually present important differences in their stability and color properties in relation to those of their anthocyanin precursors.[6−8] Thus, as a consequence of wine aging, the reddish-blue color of young red wine changes to the reddish-brown color of matured wine.

Anthocyanins can be involved in different kinds of reactions during wine aging. Condensation of anthocyanins with flavanols either directly[8,9] or by mediation of acetaldehyde[10−12] or other compounds[13] leads to new pigments that show bathochromic shifts in their visible absorption maxima in relation to native anthocyanins. Anthocyanins also undergo cycloaddition reactions with wine constituents possessing a polarized double bond, such as the enol forms of pyruvic acid[14,15] and acetaldehyde,[16,17] vinylphenol,[18] hydroxycinnamic acids,[19] or the enol form of acetone,[17,20] which lead to the so-called pyranoanthocyanins. The colors of this type of pigment are more stable against pH increase and bisulfite bleaching than those of the native anthocyanins and exhibit an orange-red hue as a consequence of a hypsochromic shift in their visible absorption maxima.[15,16,19,21] Moreover, anthocyanins have been proven to be involved in direct condensation reactions with certain *C*-glucosidic ellagitannins,[22,23] oak compounds that are present in wines as a consequence of their aging process in contact with oak wood. Such *C*-glucosidic ellagitannins are hydrolyzable tannins that may represent up to 10% of dry oak heartwood weight.[24] The most representative structures of these ellagitannins are the monomeric forms vescalagin and castalagin, two epimers first isolated and characterized by Mayer.[25] Lyxose/xylose derivatives (grandinin and roburin E, respectively) and dimeric forms (roburins A, B, C, and D) have also been described.[26,27] Some of these ellagitannins may take part in the changes of color during wine maturation and aging, helping to improve the stability of the wine color and also protecting it against oxidation.[28−30] However, among those *C*-glucosidic ellagitannins only the vescalagin has been proven to directly react with other wine components such as (epi)-catechin, malvidin, and oenin (malvidin 3-*O*-glucoside).[22,23,31,32] The reaction with these anthocyani(di)ns leads to new hybrid pigments that show a purple hue in accordance with the important bathochromic shift in the absorption band of their visible spectra.[22,23] These hybrid pigments have also shown differences in their behavior against changes in pH values in relation to native anthocyanins.

In a mildly acidic aqueous solutions such as wine, anthocyanins and related compounds are involved in a series of pH-dependent chemical reactions leading to both colored and colorless species as shown in Figure 1 for myrtillin (delphinidin 3-*O*-glucoside). The network of pH-dependent

Received: July 30, 2013
Revised: October 25, 2013
Accepted: October 29, 2013
Published: October 29, 2013

dx.doi.org/10.1021/jf403319u | J. Agric. Food Chem. 2013, 61, 11569−11578

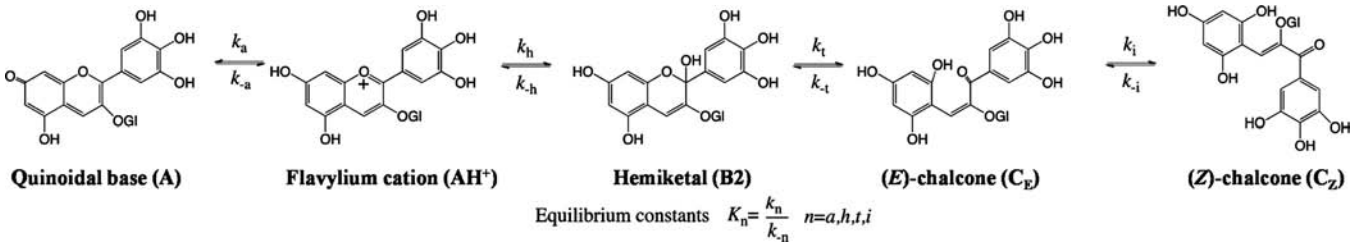

Figure 1. Network of pH-dependent equilibrium of myrtillin in acidic medium.

chemical reactions involving anthocyanins is well established.[33−38] Depending on the pH, these compounds can exist in the form of different species in equilibrium through proton transfer, hydration, tautomerization, and isomerization reactions, although this last occurs to a lesser extent. The flavylium cation $\mathbf{AH}^+$ is the predominant species in the equilibrium under sufficiently acidic conditions (pH <2). When the pH is raised, the flavylium cation is involved in two parallel reactions: (i) deprotonation to form the blue-purple quinoidal base **A** (kinetic product) and (ii) hydration in position 2 of the pyrylium nucleus to give the colorless hemiketal **B2** (thermodynamic product), herein referred to as **B**. This species leads by a ring-opening tautomeric process to the (*E*)-chalcone ($\mathbf{C_E}$), which in turn can be transformed via isomerization into the (*Z*)-chalcone ($\mathbf{C_Z}$).

At equilibrium, the network can be very simplified if the system is considered as a single acid−base equilibrium between the flavylium cation and a conjugate base **CB**, defined by the apparent acidity constant K'_a, eq 1:

$$\mathbf{AH}^+ + H_2O \rightleftharpoons \mathbf{CB} + H_3O^+ \quad K'_a = K_a + K_h + K_hK_t + K_hK_tK_i \tag{1}$$

CB is defined as the sum of the concentrations of the other species in the network, $[\mathbf{CB}] = [\mathbf{A}] + [\mathbf{B}] + [\mathbf{C_E}] + [\mathbf{C_Z}]$. This global equilibrium is decomposed into its corresponding components, eqs 2−5:

$$\mathbf{AH}^+ + H_2O \rightleftharpoons \mathbf{A} + H_3O^+ \quad K_a \text{ proton transfer} \tag{2}$$

$$\mathbf{AH}^+ + 2H_2O \rightleftharpoons \mathbf{B} + H_3O^+ \quad K_h \text{ hydration} \tag{3}$$

$$\mathbf{B} \rightleftharpoons \mathbf{C_E} \quad K_t \text{ tautomerization} \tag{4}$$

$$\mathbf{C_E} \rightleftharpoons \mathbf{C_Z} \quad K_i \text{ isomerization} \tag{5}$$

Prior to reaching thermodynamic equilibrium, kinetic processes lead to the formation of transient species. When the pH rises, base **A** is immediately formed from $\mathbf{AH}^+$ as a kinetic product and later totally or partially disappears to yield the thermodynamic equilibrium in which at least some of the other species (**B**, $\mathbf{C_E}$, or $\mathbf{C_Z}$) are more stable than **A**.[33]

The relative distribution of the mole fraction of each of these species in the conjugate base, **CB**, is dependent on the substitution pattern of the flavylium core.[36,39] In the case of anthocyanins, the hemiketal **B** is the major component and the quinoidal base **A** and the (*E*)- and (*Z*)-chalcones are the minor species.[36]

The thermodynamic and kinetic parameters of some anthocyanin-derived pigments have been studied showing important differences in relation to the native anthocyanins.[7,19,40] These differences depend on the type of substituent linked to the native anthocyanins. In particular, the anthocyanin−ellagitannin hybrid pigment previously studied by Dangles, Quideau, and co-workers,[22] 1-deoxyvescalagin-(1β→8)-oenin, has been shown to be a more stable pigment than oenin with respect to hydration.

In this work, the thermodynamic and kinetic constants of the network of a new related anthocyanin−ellagitannin hybrid pigment, 1-deoxyvescalagin-(1β→8)-myrtillin (Figure 2) have been determined and compared to those of myrtillin to evaluate the changes in the aqueous equilibria of myrtillin induced by the vescalagin substitution at the carbon C-8′ of the flavanic skeleton.

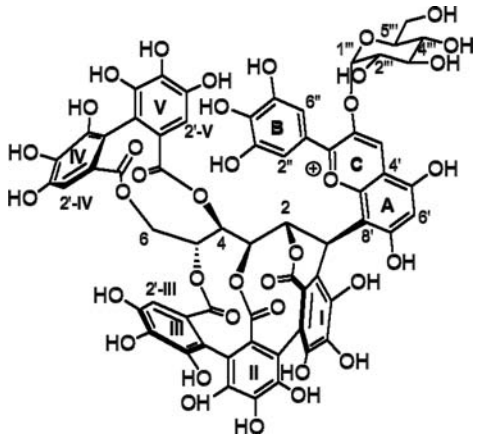

Figure 2. Structure of myrtillin−vescalagin hybrid pigment (1-deoxyvescalagin-(1β→8)-myrtillin).

MATERIALS AND METHODS

Chemicals. Myrtillin (delphinidin 3-*O*-glucoside) was extracted from the skins of *Vitis vinifera* L. cv. Tempranillo grapes using a previously developed methodology.[41] 1-Deoxyvescalagin-(1β→8)-myrtillin (*Vg-Myr*) hybrid pigment has been previously hemisynthetized, purified by semipreparative HPLC (final purity > 95%), and characterized by HPLC-DAD, mass spectrometry, and NMR.[41]

The solutions were prepared in Millipore water. A universal buffer of Theorell and Stenhagen[42] was made by dissolving 2.25 mL of phosphoric acid (85% w/w), 7.00 g of monohydrated citric acid, 3.54 g of boric acid, and 343 mL of 1 M NaOH solution in Millipore water to 1 L. The pH of the pigment solutions was adjusted by the addition of HCl, NaOH, or the universal buffer of Theorell and Stenhagen at the appropriate pH value and was measured on a Radiometer Copenhagen PHM240 pH/ion meter (Radiometer Analytical, Lyon, France).

Stock solution of the 1-deoxyvescalagin-(1β→8)-myrtillin pigment (0.15 mM) was prepared in aqueous solution of 0.1 M HCl, which was kept protected against sunlight at 4 °C. The resulting low pH value of the stock solutions (pH ≈1) ensured that most of the pigment is in its flavylium form, thus preventing pigment degradation. All of the solvents employed were of analytical grade.

Absorption Spectroscopy. UV−visible absorption spectra were recorded using Varian-Cary 100 Bio and Varian-Cary 5000 spectrophotometers (Agilent Technologies, Waldbronn, Germany). Spectroscopic absorbance curves were recorded from 200 to 800 nm

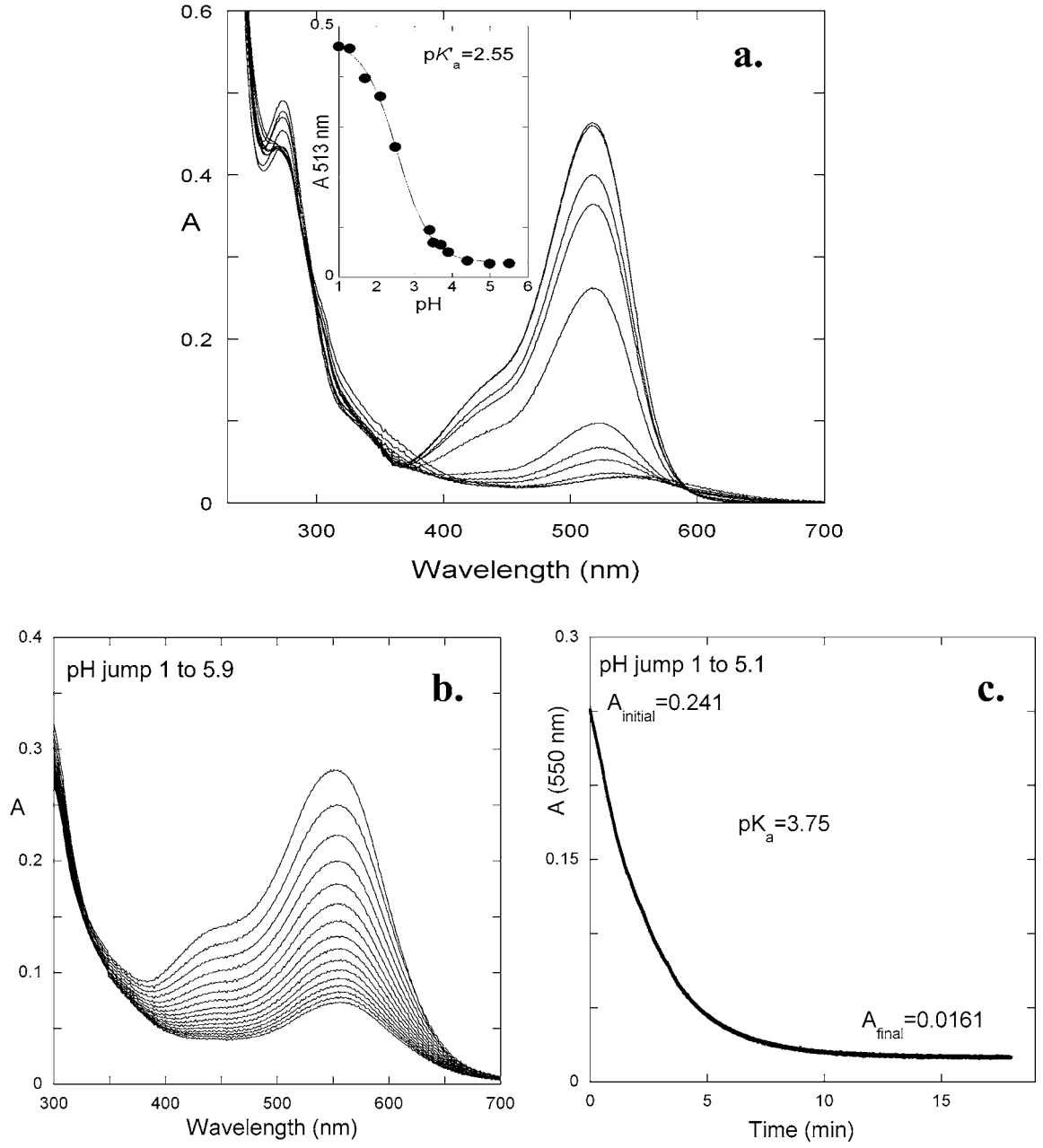

Figure 3. (a) Absorption spectra of equilibrated solutions of myrtillin 5×10^{-5} M (universal buffer 0.03 M) at different pH values; (inset) determination of pK'_a using the absorbance at 513 nm. (b) Spectral variations of a solution of myrtillin 5×10^{-5} M (universal buffer 0.03 M) upon a pH jump from 1 to 5.9. (c) Trace of the absorbance of a solution of myrtillin 5×10^{-5} M (universal buffer 0.03 M) at 550 nm upon a pH jump to 5.1.

with a 1 nm sampling interval using a quartz cell cuvette of 3.5 mL capacity and 1 cm optical path for all of the solutions. Stopped-flow experiments were conducted in an Applied Photophysics SX20 stopped-flow spectrometer (Applied Photophysics Ltd., Leatherhead, UK) provided with a PDA.1/UV photodiode array detector with a minimum scan time of 0.65 ms and a wavelength range of 200−735 nm.

Determination of the Thermodynamic and Kinetic Parameters. The network of chemical reactions was studied at pH values between 1 and 6. The apparent acidity constant (K'_a) was accomplished by measuring, on the UV−visible spectrophotometer, equilibrated solutions composed of one-third of the corresponding pigment stock solution, one-third of a solution of 0.1 M NaOH, and one-third of a universal buffer solution adjusted at different pH values (1.0, 1.3, 1.7, 2.1, 2.5, 3.4, 3.5, 3.7, 3.9, 4.4, 5.0, and 5.5 in the case of myrtillin and 1.0, 1.6, 2.0, 2.5, 3.0, 3.3, 4.1, 4.2, and 4.7 in the case of *Vg-Myr*). The pH of the solutions was also measured after a spectroscopic absorbance curve had been recorded.

Kinetic and thermodynamic constants were determined using the so-called direct and reverse pH jump experiments: The spectral variations after a pH jump from equilibrated solutions of the pigment were followed over time by conventional UV−vis spectroscopy or by stopped-flow coupled to a UV−vis detector depending on the rate of the monitored process.

RESULTS AND DISCUSSION

The thermodynamics and kinetics of the network of chemical reactions (Figure 1) involving myrtillin and the *Vg-Myr* hybrid pigment have been studied using the same experimental procedure to allow comparisons of the data under identical conditions.

dx.doi.org/10.1021/jf403319u | J. Agric. Food Chem. 2013, 61, 11569−11578

The network simplification considering it as a single acid−base equilibrium between the flavylium cation and a conjugate base **CB**, eq 1, is useful for the analysis of the thermodynamic equilibria. Moreover, considering that in the case of anthocyanins the formation of the (*Z*)-chalcone from the (*E*)-chalcone is the slowest process, further simplifications can be done in the single acid−base equilibrium, defining a pseudoequilibrium involving all other species, eq 6.

$$\mathbf{AH}^+ + H_2O \rightleftharpoons \mathbf{CB}^{\wedge} + H_3O^+ \quad K_a^{\wedge} = K_a + K_h + K_hK_t \tag{6}$$

$$[\mathbf{CB}^{\wedge}] = [\mathbf{A}] + [\mathbf{B}] + [\mathbf{C_E}]$$

Taking into account the equilibria shown in Figure 1 and eqs 1−6, it is easy to establish the expressions to determine the pH-dependent mole fraction distribution of the network species both at equilibrium and at pseudoequilibrium if K'_a is substituted by $K_a^{\wedge}$ eq 7.

$$\chi_{AH^+} = \frac{[H^+]}{[H^+] + K'_a};\ \chi_A = \frac{K_a}{[H^+] + K'_a};\ \chi_B = \frac{K_h}{[H^+] + K'_a};$$
$$\chi_{C_E} = \frac{K_hK_t}{[H^+] + K'_a};\ \chi_{C_Z} = \frac{K_hK_tK_i}{[H^+] + K'_a} \tag{7}$$

A way to study the kinetics processes of the network is to carry out different pH jumps from equilibrated solutions of the pigment to higher (direct)[34] or lower (reverse)[43] pH values. In the case of anthocyanins the direct pH jumps give rise to three different kinetic processes. The first one is the deprotonation to form the quinoidal base, **A**, the fastest kinetic step of the network, eq 8, which can be detected only through very fast techniques such as temperature jumps.[35]

$$k_{1st} = k_a + k_{-a}[H^+] \tag{8}$$

The second one is the hydration taking place according to eq 9:

$$k_{2nd} = \frac{[H^+]}{[H^+] + K_a}k_h + \frac{1}{1 + K_t}k_{-h}[H^+] \tag{9}$$

Equation 9 presupposes that the tautomerization reaction (C-ring-opening−closure) is much faster than hydration, which is usually true if the final pH is >2. However, if the final pH value is <2, the hydration becomes the fastest process. At this point the species $\mathbf{AH}^+$, **A**, **B**, and $\mathbf{C_E}$ are in pseudoequilibrium. Finally, the system equilibrates through a much slower process to form $\mathbf{C_Z}$, eq 10, a minor species in the case of anthocyanins.

$$k_{3rd} = \frac{K_hK_t}{[H^+] + K_a + K_h(1 + K_t)}k_i + k_{-i} \tag{10}$$

In the case of the reverse pH jumps, if the final pH is sufficiently acidic, the hydration becomes the fastest process and $\mathbf{AH}^+$ is formed from **B** in a first step, and in a second process additional $\mathbf{AH}^+$ is obtained from $\mathbf{C_E}$ through **B**. Equations 11 and 12 account for these two processes. The acid and basic catalyses were not included in eq 12 because its influence on the tautomerization can be neglected.[44]

$$k_{obs\ (hydration)} = \frac{[H^+]}{K_a + [H^+]}k_h + k_{-h}[H^+] \tag{11}$$

$$k_{obs\ (taut)} = k_{-t} \tag{12}$$

Thermodynamic and Kinetic Parameters of Myrtillin. In a previous paper,[43] the network of chemical reactions of myrtillin was studied. Here, some experiments are reproduced for comparison purposes with *Vg-Myr*. Initially, the thermodynamics of the network was studied. Figure 3a shows the spectral variations of myrtillin solutions at different pH values upon equilibration (overnight) and the fitting of the data set to calculate the pK'_a (Figure 3a, inset). The concentration used is sufficiently low to prevent self-aggregation.[43] The myrtillin pK'_a (Table 1) was calculated by fitting the absorbance values at the maximum absorbance wavelength of the flavylium cation (513 nm) for a single acid−base equilibrium according to eq 1. The value obtained ($pK'_a = 2.55$) is in good agreement with the one previously reported.[43] Inspection of this figure shows the disappearance of the characteristic flavylium cation absorption as the pH is raised. It can also be observed that, at pH >4, the equilibrium is essentially constituted by a species absorbing in the UV region of the spectra. Moreover, a remaining absorption in the visible is easily attributed to the quinoidal base **A**, which is present at equilibrium.

Table 1. Equilibrium Constants

	pK'_a	pK_a	K_h (M^{-1})[a]	K_t[b]	K_i
Myr	2.5(5) ± 0.05	3.7(5) ± 0.05	2.8×10^{-3}	0.06	0.2[c]
Vg-Myr	2.2(5) ± 0.05	2.9 ± 0.05	2.4×10^{-3}	0.9	0.3[c]

[a]Estimated error 5%. [b]Estimated error 20%. [c]The value is a rough estimate.

The spectral variations upon a direct pH jump from an equilibrated solution at pH 1 to pH 5.9 are represented in Figure 3b, showing the disappearance of the quinoidal base (which is formed immediately after the pH jump) to give the pseudoequilibrium, that is, a (pseudo)equilibrium involving all of the forms of the flavylium network except the (*Z*)-chalcone. In Figure 3c, the fitting obtained at 550 nm upon a similar pH jump from pH 1.0 to 5.1 is shown: (i) initially, almost all the flavylium cation is transformed into quinoidal base **A**; (ii) the final absorbance at 550 nm (at equilibrium, not shown) is due to the remaining quinoidal base; (iii) the absorbance at 550 nm at pseudoequilibrium (20 min) is very similar to the one at equilibrium (a few hours) as a consequence of the very small mole fraction of $\mathbf{C_Z}$ at equilibrium. On this basis, the ratio $A_{final}/A_{initial} = K_a/K'_a$ allows the calculation of $pK_a = 3.75$.[45] The value of the pK_a obtained is in accordance with previous studies.[43]

Previously, reverse pH jump experiments of myrtillin followed by stopped flow were reported[43] and are here presented for comparison purposes. The spectral variations upon a reverse pH jump from an equilibrated solution of myrtillin at pH 4.5 to 1.4 are shown in Figure 4a. Inspection of this figure shows the rising of the flavylium absorption and the existence of three distinct processes. The initial absorption appears during the mixing time of the stopped flow and is due to the protonation of the quinoidal base (**A**) leading to the flavylium cation ($\mathbf{AH}^+$). From this point, the process is biexponential (Figure 4b). The fitting of the absorbance at 512 nm for a biexponential equation allowed the calculation of the kinetic and thermodynamic constants of the tautomerization process. The faster process ($k_{1obs} = 1.2\ s^{-1}$) corresponds to the flavylium formation through the hemiketal (**B**) previously available at pH 4.5 (see eq 11). This step is followed by a slower one ($k_{2obs} = 0.3\ s^{-1}$) that is due to the formation of more flavylium cation from (*E*)-chalcone ($\mathbf{C_E}$) via the transient hemiketal (**B**). Because the final pH of the reverse pH jump is sufficiently acidic, hydration is the fastest process and the kinetic constant determined in the second step k_{2obs}

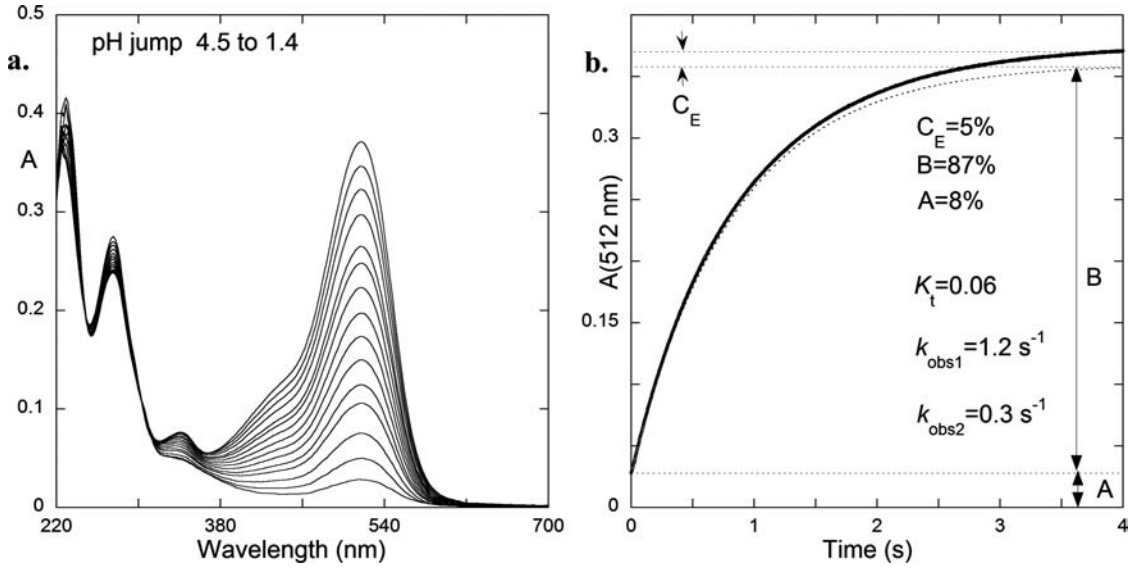

Figure 4. (a) Spectral variations upon a reverse pH jump from equilibrated solutions of myrtillin 2×10^{-5} M at pH 4.5 back to 1.4 obtained by stopped flow. (b) Trace taken at 512 nm; from the ratio of the amplitudes of the two exponential processes $\mathbf{C_E}/\mathbf{B}$, K_t = 0.06, is calculated. As a consequence of the experimental error associated with the values of the equilibrium and rate constants the calculation of the fraction of **CB** species is slightly higher than 100%. (Figures reprinted from *Phytochemistry*, Vol. 83, Y. Leydet et al., "The effect of self-aggregation on the determination of the kinetic and thermodynamic constants of the network of chemical reactions in 3-glucoside anthocyanins", pp. 125−135, Copyright (2012), with permission from Elsevier).

Table 2. Rate Constants

	k_h (s^{-1})[a]	k_{-h} (M^{-1} s^{-1})[a]	k_t (s^{-1})[b]	k_{-t} (s^{-1})[b]	k_i (s^{-1})	k_{-i} (s^{-1})
Myr	0.09	32	0.02 (pH 1.4)	0.30	5.1×10^{-5}[c]	2.4×10^{-4}[c]
Vg-Myr	0.065	25	0.76 (pH 0.7)	0.84	7.9×10^{-5}[c]	2.7×10^{-4}[c]

[a]Estimated error 5%. [b]Estimated error 20%. [c]The value is a rough estimate.

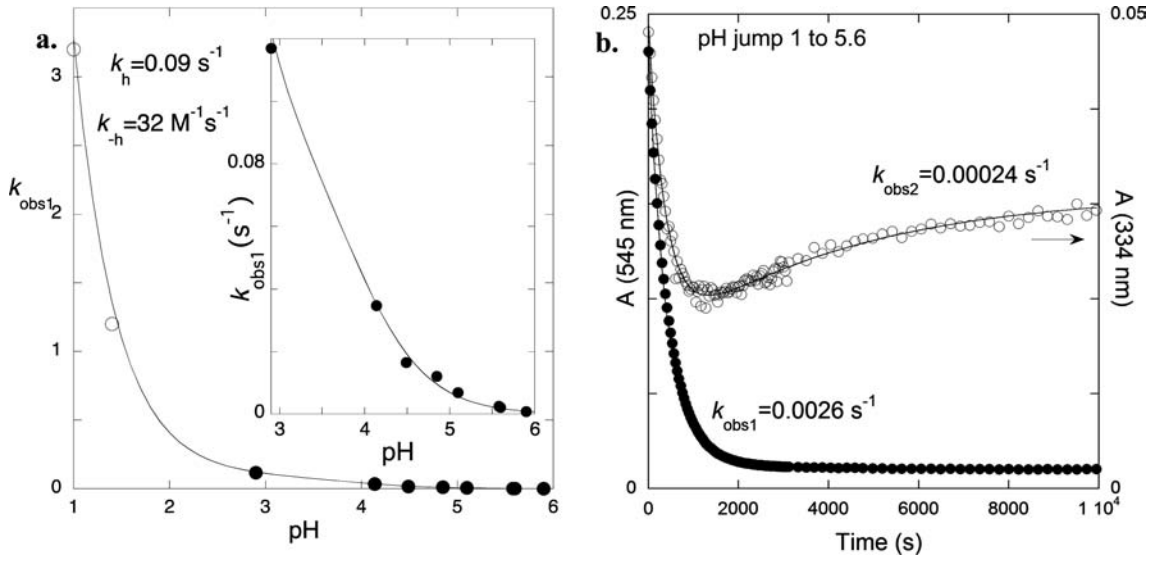

Figure 5. (a) Representation of the hydration rate constant as a function of pH fitted by means of eq 9 (direct pH jumps (●), magnified in the inset) and eq 11 (reverse pH jumps (○)). Both fittings are coincident due to the low value of K_t. (b) Trace of absorbance at 545 nm (●) and at 334 nm (○) of myrtillin 2×10^{-5} M upon a pH jump from 1 to 5.6. (Reprinted from *Phytochemistry*, Vol. 83, Y. Leydet et al., "The effect of self-aggregation on the determination of the kinetic and thermodynamic constants of the network of chemical reactions in 3-glucoside anthocyanins", pp. 125−135, Copyright (2012), with permission from Elsevier).

corresponds to k_{-t} (eq 12). The amplitudes of the two exponentials give the ratio $[\mathbf{C_E}]/[\mathbf{B}] = K_t = 0.06$ (eq 4). From the values of K_t and k_{-t}, the direct kinetic constant k_t of the tautomerization process can be calculated (Table 2). Inspection of Figure 4b corroborates that at pH 4.5 the hemiketal is the predominant form, whereas the fractions of the quinoidal base **A** and the (*E*)-chalcone $\mathbf{C_E}$ are very small.

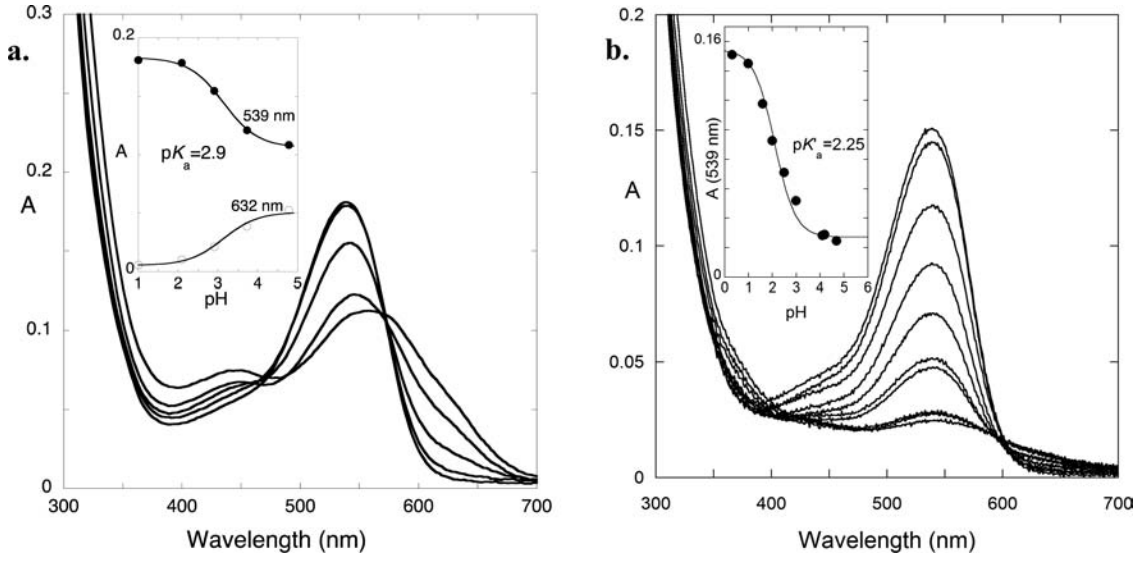

Figure 6. (a) Absorption spectra of *Vg-Myr* obtained 6 ms after a pH jump from equilibrated solutions of *Vg-Myr* 2×10^{-5} M at pH 1.0 to higher pH values, followed by stopped flow; (inset) determination of pK_a using the absorbance at 539 nm ($\mathbf{AH^+}$) and at 632 nm (**A**). (b) Absorption spectra of equilibrated solutions of *Vg-Myr* 2×10^{-5} M (universal buffer 0.03 M) at different pH values; (inset) determination of pK'_a using the absorbance at 539 nm.

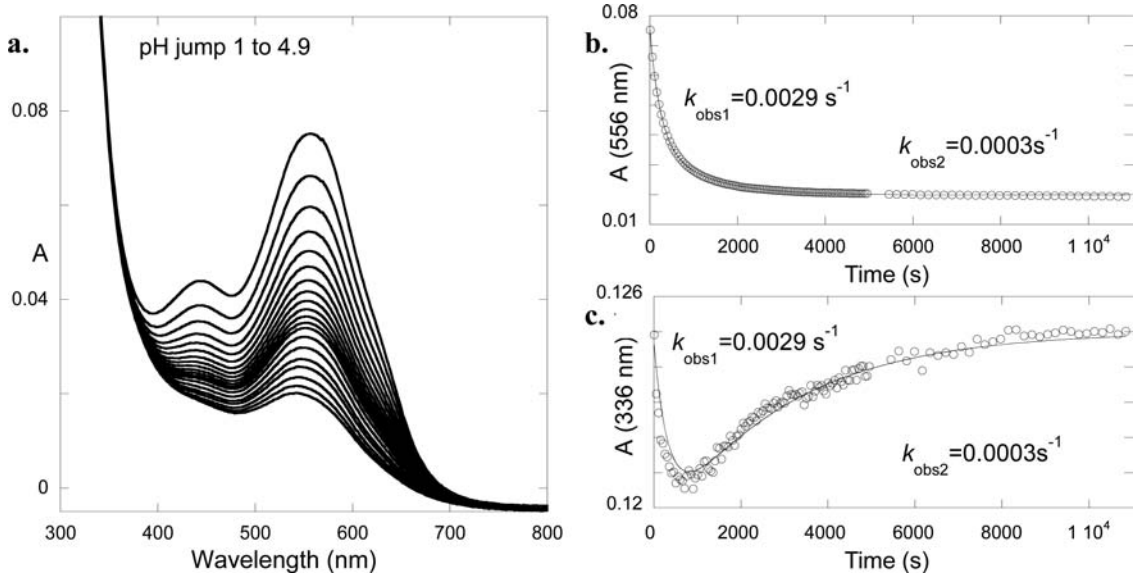

Figure 7. (a) Spectral variations of a solution of *Vg-Myr* 2×10^{-5} M upon a direct pH jump from pH 1 to 4.9. (b) Trace of the absorbance at 556 nm upon the same direct pH jump monitoring the disappearance of the quinoidal base. (c) Trace of the absorbance at 336 nm upon the same direct pH jump monitoring the formation of (*Z*)-chalcone.

More information regarding the system can be achieved by monitoring the kinetics of the direct pH jumps. In this case, equilibrium is reached by two consecutive processes, each one following a first-order reaction. Due to the fact that these two kinetic processes are well separated in time, it is possible to analyze them independently. In Figure 3c, only the first step (hydration control) is observed. A series of direct pH jumps of myrtillin solutions at pH 1.0 to higher pH values were carried out. Representation of the rate constants of this step (k_{1obs}) as a function of pH (eq 9) is depicted in Figure 5a. In the same figure, the kinetic constants determined for the fast process of the reverse pH jumps, that is, k_{1obs} (Figure 4b) have also been added, because in both cases the rate-determining step of the kinetics is the hydration (eq 11). Due to the low value of K_t, fitting of the data using eqs 9 and 11 is identical within experimental error, leading to $k_h = 0.09\ s^{-1}$ and $k_{-h} = 32\ M^{-1}\ s^{-1}$. From the ratio of these kinetic constants, $K_h = 2.8 \times 10^{-3}\ M^{-1}$ was calculated.

Finally, Figure 5b represents the two processes following a direct pH jump (to pH 5.6). The first one shows the disappearance of **A** by two consecutive steps, both following first-order kinetics laws. The second process reveals, through the spectral variations at 334 nm, the formation of the (*Z*)-chalcone.[43] As previously mentioned, the mole fraction of $\mathbf{C_Z}$ at equilibrium is very low, as confirmed by the small rise of the absorbance at this wavelength. From all of the thermodynamic data determined (K'_a, K_a, K_h, and K_t) it was possible to give a rough value for $K_i = 0.2$ by using eq 1. Finally, by means of eq 10 and using the rate of the slowest kinetic process of the pH jump shown in Figure 5b ($k_{2obs} = 0.00024\ s^{-1}$), it was also

dx.doi.org/10.1021/jf403319u | J. Agric. Food Chem. 2013, 61, 11569−11578

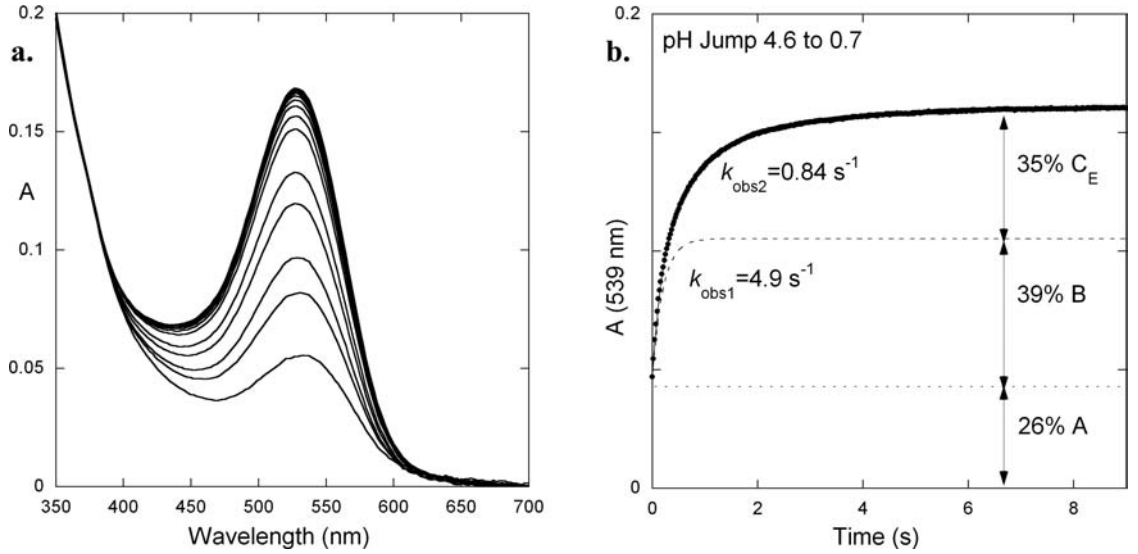

Figure 8. (a) Spectral changes of a solution of *Vg-Myr* 2×10^{-5} M upon a reverse pH jump from equilibrated solutions at pH 4.6 to pH 0.7. (b) Trace of the absorption at 539 nm according to the biexponential growth. From the ratio $\mathbf{C_E}/\mathbf{B}$, $K_t = 0.9$.

possible to estimate the isomerization rate constants $k_i = 5.1 \times 10^{-5}$ s^{-1} and $k_{-i} = 2.4 \times 10^{-4}$ s^{-1}. All of the data of the equilibrium and rate constants determined for the myrtillin network are collected in Tables 1 and 2.

Thermodynamic and Kinetic Parameters of 1-Deoxyvescalagin-(1β→8)-myrtillin. In the case of 1-deoxyvescalagin-(1β→8)-myrtillin (*Vg-Myr*), the pK_a was directly determined by stopped flow, from the absorption spectra of solutions of *Vg-Myr* 2×10^{-5} M corresponding to 6 ms after several direct pH jumps from pH 1 to higher pH values (Figure 6a). The equilibrium was studied using the variations in the absorbance at 539 nm, corresponding to the flavylium form, and in the absorbance at 632 nm, corresponding to the quinoidal base. The absorbance at these wavelengths was plotted versus pH (Figure 6a, inset). The fitted data are compatible with the single acid−base equilibrium $\mathbf{AH^+}/\mathbf{A}$ (eq 2), with pK_a = 2.9. This value shows that the hybrid pigment has higher acidity than the native myrtillin (Table 1). The lower pK_a value in the case of *Vg-Myr* might be a consequence of a reduction of the flavylium electronic density due to the vescalagin substitution at carbon C-8′ of the flavanic skeleton.

The spectral variations of *Vg-Myr* 2×10^{-5} M solutions at different pH values upon equilibration (overnight) are presented in Figure 6b. It can be noted that the final equilibrium of *Vg-Myr* is qualitatively similar to the one of myrtillin shown in Figure 3a. The calculation of pK'_a was done by fitting the absorbance values at the maximum absorbance wavelength of the flavylium cation (539 nm) for a single acid−base equilibrium according to eq 1. The pK'_a calculated for *Vg-Myr* is smaller than that determined for myrtillin (Table 1), an indication that the flavylium cation is slightly destabilized in *Vg-Myr*.

Figure 7a shows the spectral variations upon a pH jump from an equilibrated solution of *Vg-Myr* 2×10^{-5} M at pH 1−4.9. As in the case of myrtillin, the disappearance of **A** takes place in two steps that can be studied separately: the first one leads to the pseudoequilibrium involving all of the species of the network except $\mathbf{C_Z}$, and the second one corresponds to the formation of a small amount of $\mathbf{C_Z}$. The first process (Figure 7b) can be studied using the absorbance at 556 nm to follow the disappearance of the quinoidal base **A**. Taking into account the initial and final absorbances at 556 nm, it is also possible to calculate the value of K_a by means of the equation $A_{final}/A_{initial} = K_a/K'_a$, giving $K_a = 10^{-2.8}$, very close to the value obtained by stopped flow (Table 1; see also Figure 6a). The direct pH jump also allowed the study of the second process, in which the formation of (*Z*)-chalcone can be observed, by tracing the absorbance at 336 nm as a function of time (Figure 7c).

Important information is obtained by means of reverse pH jumps from equilibrated solutions. Figure 8a shows the spectral variations of a solution of *Vg-Myr* 2×10^{-5} M upon a reverse pH jump from pH 4.6 to 0.7. As in the case of myrtillin, the existence of three different processes could be noted (Figure 8b). The initial absorbance immediately after the pH jump corresponds to the fraction of **A** present at the initial pH, because at pH 4.6 the mole fraction of $\mathbf{AH^+}$ can be neglected by taking into account the low value of pK'_a (Table 1). The variation of the absorbance at 539 nm follows a biexponential curve. Using the same approach reported above for myrtillin, $k_{1obs} = 4.9$ s^{-1} should be fitted with eq 11, and $k_{2obs} = 0.84$ s^{-1} gives k_{-t} (eq 12). Moreover, from the ratio of the amplitudes of the two exponentials, $[\mathbf{C_E}]/[\mathbf{B}] = K_t = 0.9$ was calculated. Using the values of K_t and k_{-t}, the direct kinetic constant of the tautomerization process k_t can be calculated by the following expression: $K_t = k_t/k_{-t}$ (Table 2). The value of K_t obtained is significantly higher than the one obtained for myrtillin. This fact reveals that the ring opening is more favorable in *Vg-Myr* compared with myrtillin. It seems that the anthocyanidin greatly influences the thermodynamic and kinetic properties of the anthocyanin−ellagitannin hybrid pigment, because for myrtillin−vescalagin pigment, the constants of acidity and tautomerization are very different from those of myrtillin, whereas there are no differences between the values of these constants of oenin−vescalagin hybrid pigment in relation to those of oenin.[22]

Taking into account that the mole fraction of $\mathbf{C_Z}$ is very small, the approximation $[\mathbf{CB}] = [\mathbf{CB^\wedge}]$ (eq 6) can be done and the mole fraction of the hemiketal gives the ratio $[\mathbf{B}]/[\mathbf{CB^\wedge}] = K_h/K'_a = 0.39$, and therefore the value of $K_h = 2.5 \times 10^{-3}$ M^{-1} is estimated. Inspection of Figure 8b also shows the proportion of the different forms of *Vg-Myr*. In this case, the hemiketal (colorless) represents a lower percentage than in the case of

dx.doi.org/10.1021/jf403319u | *J. Agric. Food Chem.* 2013, 61, 11569−11578

myrtillin (Figure 4b), whereas the quinoidal base (blue) and the (*E*)-chalcone (yellowish) represent higher percentages in *Vg-Myr* than in the native anthocyanin.

As shown above, additional information is obtained by representing the pH dependence of the observed rate constants of hydration control (k_{1obs}) in both direct and reverse pH jumps (Figure 9). In the case of *Vg-Myr*, as a consequence of the higher value of K_t compared with that for myrtillin, data should be fitted using two different equations. Equation 9 should be used to fit the rates of direct pH jumps, because the tautomerization process is faster than hydration when the final pH is >2. The rates obtained in reverse pH jumps should be in turn fitted using eq 11, because the hydration process is now the fastest one. The simultaneous fitting of the rates using these equations allowed the calculation of $k_h = 0.065\ s^{-1}$ and $k_{-h} = 27\ M^{-1}\ s^{-1}$ leading to $K_h = 2.4 \times 10^{-3}\ M^{-1}$, in good agreement with the value calculated from the reverse pH jumps ($K_h = 2.5 \times 10^{-3}\ M^{-1}$) using the data shown in Figure 8b.

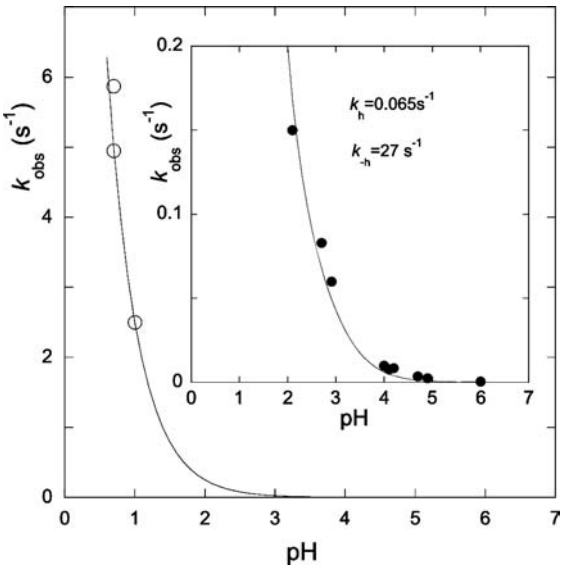

Figure 9. Representation of the hydration rate constant as a function of pH: (●) direct pH jumps from equilibrated solutions at pH 1 to higher pH values; (○) reverse pH jumps from equilibrated solutions at pH 4.6 to lower pH values. Fitting was achieved with eqs 9 and 11, respectively.

Knowing the values K'_a, K_a, K_h, and K_t, and taking into account eq 1, it is possible to give a value for $K_i = 0.3$. Finally, by means of the slowest rate of the kinetic process upon the pH jump shown in Figure 7b,c ($k_{2obs} = 0.0003\ s^{-1}$), eq 10, and the value of K_i, a system of two equations with two unknowns permits one to calculate $k_i = 7.9 \times 10^{-5}\ s^{-1}$ and $k_{-i} = 2.7 \times 10^{-4}\ s^{-1}$. The value obtained for the thermodynamic constant of the isomerization process is similar to the one obtained for myrtillin. This fact can also be observed for the rate constants of the isomerization process. The data of the equilibrium and rate constants of *Vg-Myr* are collected in Tables 1 and 2.

Figure 10 shows the energy level diagram of myrtillin (a) and *Vg-Myr* (b) in order to illustrate the thermodynamic situation of both networks.[45] Inspection of the diagram clearly shows that the quinoidal base (**A**) and the (*E*)-chalcone ($\mathbf{C_E}$) in *Vg-Myr* are noticeably stabilized in comparison with myrtillin, whereas **B** is slightly destabilized. Dangles, Quideau, and co-workers have demonstrated for the oenin−vescalagin hybrid pigment, by means of NMR experiments,[22] a spatial proximity between the B-ring proton (6″-H) of the anthocyanin and the 1-H and 2-H protons of the vescalagin moiety (Figure 2). Thus, a possible explanation of the stabilization of **A** is the existence

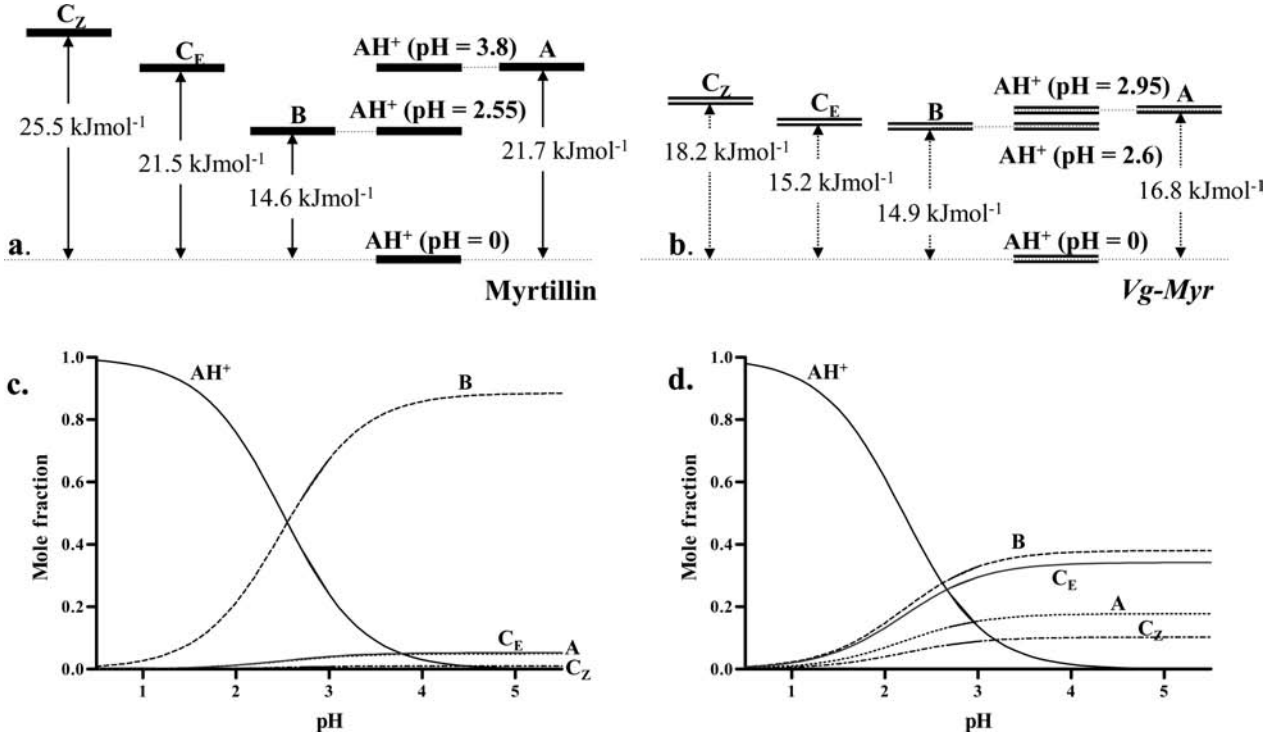

Figure 10. (Upper) Energy level diagrams of myrtillin (a) and *Vg-Myr* (b). (Bottom) Mole fraction distribution depending on the pH of myrtillin (c) and *Vg-Myr* (d).

of a less polar environment involving the myrtillin moiety of *Vg-Myr*. Moreover, in the case of *Vg-Myr*, if the pH is raised from acidic pH to 2.6, the $\mathbf{AH}^+$ will equilibrate with **B**, which in turn will equilibrate with $\mathbf{C}_E$ given that at pH values up to 2.6, (*E*)-chalcone is almost as stabilized as the hemiketal **B**. Because the vescalagin substitution at carbon C-8′ of the myrtillin might affect the electronic density of the anthocyanin, (*E*)-chalcone might be stabilized as a consequence of the electron delocalization in its structure.

The mole fraction distributions depending on the pH of the myrtillin (Figure 10c) and the *Vg-Myr* (Figure 10d) were calculated by means of eq 7, and the data are reported in Table 1. As can be seen, when the pH rises, the mole fraction of $\mathbf{AH}^+$ decreases concomitantly with an increase of the remaining species of the network. The apparent acidity of $\mathbf{AH}^+$ is slightly higher in *Vg-Myr*, as indicated by the lower value of pK'_a (Table 1). Moreover, the increase of mole fractions of **A**, $\mathbf{C}_E$, and $\mathbf{C}_Z$ at the expense of **B** is significant in *Vg-Myr*.

The differences in the mole fraction distributions between *Vg-Myr* and myrtillin can affect the color of the slightly acidic solutions of theses pigments. In the case of myrtillin, at pH >3.5, the major species is the hemiketal and the solutions become almost colorless. The solutions of the hybrid pigment at these pH values are colored, because the mole fraction corresponding to the yellowish chalcones (mainly $\mathbf{C}_E$) and to the blue quinoidal base are higher.

It is worthy of note that the high mole fraction of $\mathbf{C}_E$ in mildly acidic media may explain why in this media *Vg-Myr* (1-deoxyvescalagin-(1β→8)-myrtillin) is involved in a regioisomerization process also implicating 1-deoxyvescalagin-(1β→6)-myrtillin.[41] This regioisomerization process takes place by the ring reclosure and dehydration after the rotation around the C-4′−C-4′*a* bond of (*E*)-chalcone. Therefore, the higher mole fraction of $\mathbf{C}_E$ of *Vg-Myr* in mildly acidic media may be a key for the establishment of this equilibrium, which is slightly shifted toward a preferred formation of 1β→8 pigment.[41] Such an effect was previously reported by Jurd and Geissman[46] for a 5,7,8,4′-tetrahydroxyflavylium salt, because the existence of a hydroxyl in position 5 (taking as reference the notation of the flavylium cation) introduces an alternative for the ring closure.

These results suggest that the vescalagin substitution at the carbon C-8′ of the flavanic skeleton of myrtillin induces important changes in the aqueous equilibria of the anthocyanin. However, Nave and co-workers[40] have reported that there are no significant modifications regarding the kinetic and thermodynamic behaviors of the oenin and the catechin−oenin pigment, indicating that the network of chemical reactions involving catechin-(4,8)-malvidin-3-glucoside is controlled by its oenin moiety. Moreover, Dangles, Quideau, and co-workers[22] have reported only significant differences in the hydration process between the network of oenin and the oenin−vescalagin hybrid pigment, Thus, it seems that the changes observed in the physicochemical properties of the pigment mainly depend on the anthocyanin.

In conclusion, the thermodynamic and kinetic constants of the network of *Vg-Myr* (1-deoxyvescalagin-(1β→8)-myrtillin) have been fully determined and compared to those determined for myrtillin. The vescalagin substitution at carbon C-8′ of myrtillin leads to lower values of pK'_a and pK_a in the hybrid pigment *Vg-Myr* relative to those for myrtillin. Thus, the flavylium cation form of *Vg-Myr* is less stabilized at pH >2 and shows higher acidity than that of myrtillin. Moreover, *Vg-Myr* has much higher values of K_t and a higher rate of ring-opening (k_t) than myrtillin. The (*E*)-chalcone form of *Vg-Myr* is therefore almost as stable as the hemiketal form at moderately acidic pH values, whereas in the case of myrtillin, the hemiketal is by far the most stabilized form at these pH values. As a consequence, in the case of myrtillin the major structural format at moderately acidic pH values (4 < pH < 6) is clearly the hemiketal **B**, whereas **A** and $\mathbf{C}_E$ are minority species. Conversely, in the case of *Vg-Myr*, the percentages of $\mathbf{C}_E$ and **A** are noticeably high. As a consequence of the differences in the mole fraction distributions between *Vg-Myr* and myrtillin, the former can provide significantly more color with a different hue in slightly acidic or neutral solutions than the native anthocyanin.

AUTHOR INFORMATION

Corresponding Authors

*(R.G.) Phone: +351 212948300, ext. 10946. Fax: +351 212948550. E-mail: r.castell@fct.unl.pt.

*(M.T.E.-B.) Phone: +34 923294537. Fax: + 34 923294515. E-mail: escriban@usal.es.

Funding

Thanks are due to the Spanish MICINN and FEDER (Project ref. AGL2008-05569-C02-01 and AGL2011-30254-C02-01), to Consolider-Ingenio 2010 Programme (ref FUNC-FOOD, CSD2007-00063), and to the Spanish Ministerio de Educación for an F.P.U. predoctoral scholarship to I.G.-E. We are also grateful to the"Fundação para a Ciência e a Tecnologia for funding through Projects PTDC/QUI-QUI/117996/2010 and PEst-C/EQB/LA0006/2013 and a postdoctoral grant SFRH/BPD/44639/2008 (R.G.).

Notes

The authors declare no competing financial interest.

REFERENCES

(1) Andersen, Ø. M.; Jordheim, M. The anthocyanins. In *Flavonoids − Chemistry, Biochemistry and Applications,*; Andersen, Ø. M., Markham, K. R., Eds.; CRC Taylor & Francis: Boca Raton, FL, 2006; pp 471−551.

(2) Ribéreau-Gayon, P.; Glories, Y.; Maujean, A.; Dubourdieu, D. *Handbook of Enology. Vol. 2: The Chemistry of Wine Stabilization and Treatments.*; Wiley: Chichester, UK, 2006.

(3) Alcalde-Eon, C.; Escribano-Bailón, M. T.; Santos-Buelga, C.; Rivas-Gonzalo, J. C. Changes in the detailed pigment composition of red wine during maturity and ageing − a comprehensive study. *Anal. Chim. Acta* **2006**, *563*, 238−254.

(4) Monagas, M.; Bartolomé, B. Anthocyanins and anthocyanins-derived compounds. In *Wine Chemistry and Biochemistry*; Moreno-Arribas, M. V., Polo, M. C., Eds.; Springer Science:: New York, 2009; pp 439−462.

(5) García-Puente Rivas, E.; Alcalde Eon, C.; Santos-Buelga, C.; Rivas-Gonzalo, J. C.; Escribano-Bailón, M. T. Behaviour and characterisation of the colour during red wine making and maturation. *Anal. Chim. Acta* **2006**, *563*, 215−222.

(6) Rentzsch, M.; Schwarz, M.; Winterhalter, P. Piranoanthocyanins − an overview on structures, occurrence, and pathways of formation. *Trends Food Sci. Technol.* **2007**, *18*, 526−534.

(7) Dueñas, M.; Salas, E.; Cheynier, V.; Dangles, O.; Fulcrand, H. UV-visible spectroscopic investigation of the 8,8-methylmethine catechin-malvidin 3-glucoside pigments in aqueous solution: Structural transformations and molecular complexation with chlorogenic acid. *J. Agric. Food Chem.* **2006**, *54*, 189−196.

(8) Salas, E.; Le Guerneve, C.; Fulcrand, H.; Poncet-Legrand, C.; Cheynier, V. Structure determination and colour properties of a new directly linked flavanol-anthocyanin dimer. *Tetrahedron Lett.* **2004**, *45*, 8725−8729.

(9) Remy, S.; Fulcrand, H.; Labarbe, B.; Cheynier, V.; Moutounet, M. First confirmation in red wine of products resulting from direct anthocyanin-tannin reactions. *J. Sci. Food Agric.* **2000**, *80*, 745−751.
(10) Rivas-Gonzalo, J. C.; Bravo-Haro, S.; Santos-Buelga, C. Detection of compounds formed through the reaction of malvidin 3-monoglucoside and catechin in the presence of acetaldehyde. *J. Agric. Food Chem.* **1995**, *43*, 1444−1449.
(11) Francia-Aricha, E. M.; Guerra, M. T.; Rivas-Gonzalo, J. C.; Santos-Buelga, C. New anthocyanin pigments formed after condensation with flavanols. *J. Agric. Food Chem.* **1997**, *45*, 2262−2266.
(12) Es-Safi, N. E.; Fulcrand, H.; Cheynier, V.; Moutounet, M. Studies on the acetaldehyde-induced condensation of (−)-epicatechin and malvidin 3-*O*-glucoside in a model solution system. *J. Agric. Food Chem.* **1999**, *47*, 2096−2102.
(13) Pissarra, J.; Lourenco, S.; González-Paramás, A. M.; Mateus, N.; Santos-Buelga, C.; de Freitas, V. Formation of new anthocyanin-alkyl/aryl-flavanol pigments in model solutions. *Anal. Chim. Acta* **2004**, *513*, 215−221.
(14) Fulcrand, H.; Benabdeljalil, C.; Rigaud, J.; Cheynier, V.; Moutounet, M. A new class of wine pigments generated by reaction between pyruvic acid and grape anthocyanins. *Phytochemistry* **1998**, *47*, 1401−1407.
(15) Romero, C.; Bakker, J. Interactions between grape anthocyanins and pyruvic acid, with effect of pH and acid concentration on anthocyanin composition and color in model solutions. *J. Agric. Food Chem.* **1999**, *47*, 3130−3139.
(16) Bakker, J.; Timberlake, C. F. Isolaion, identification, and characterization of new color-stable anthocyanins occurring in some red wines. *J. Agric. Food Chem.* **1997**, *45*, 35−43.
(17) Benabdeljalil, C.; Cheynier, V.; Fulcrand, H.; Hakiki, A.; Mosaddak, M.; Moutounet, M. Evidence of new pigments resulting from reaction between anthocyanins and yeast metabolites. *Sci. Aliments* **2000**, *20*, 203−219.
(18) Fulcrand, H.; Cameira-Dos-Santos, P. J.; Sarni-Manchado, P.; Cheynier, V.; Favre-Bonvin, J. Structure of new anthocyanin-derived wine pigments. *J. Chem. Soc., Perkin Trans. 1* **1996**, *1*, 735−739.
(19) Quijada-Morín, N.; Dangles, O.; Rivas-Gonzalo, J. C.; Escribano-Bailón, M. T. Physico-chemical and chromatic characterization of malvidin 3-glucoside-vinylcatechol and malvidin 3-glucoside-vinylguaiacol wine pigments. *J. Agric. Food Chem.* **2010**, *58*, 9744−9752.
(20) Lu, Y.; Foo, L. Y. Unusual anthocyanin reaction with acetone leading to pyranoanthocyanin formation. *Tetrahedron Lett.* **2001**, *42*, 1371−1373.
(21) Sarni-Manchado, P.; Fulcrand, H.; Souquet, J. M.; Cheynier, V.; Moutounet, M. Stability and color of unreported wine anthocyanin-derived pigments. *J. Food Sci.* **1996**, *61*, 938−941.
(22) Chassaing, S.; Lefeuvre, D.; Jacquet, R.; Jourdes, M.; Ducasse, L.; Galland, S.; Grelard, A.; Saucier, C.; Teissedre, P. L.; Dangles, O.; Quideau, S. Physicochemical studies of new anthocyano-ellagitannin hybrid pigments: about the origin of the influence of oak *C*-glycosidic ellagitannins on wine color. *Eur. J. Org. Chem.* **2010**, *1*, 55−63.
(23) Quideau, S.; Jourdes, M.; Lefeuvre, D.; Montaudon, D.; Saucier, C.; Glories, Y.; Pardon, P.; Pourquier, P. The chemistry of wine polyphenolic *C*-glycosidic ellagitannins targeting human topoisomerase II. *Chem.−Eur. J.* **2005**, *11*, 6503−6513.
(24) Scalbert, A.; Monties, B.; Favre, J. M. Polyphenols of *Quercus robur* − adult tree and *in vitro* grown calli and shoots. *Phytochemistry* **1988**, *27*, 3483−3488.
(25) Mayer, W.; Gabler, W.; Riester, A.; Korger, H. Uber die gerbstoffe aus dem holz der edelkastanie und der ieche. 2. Die isolierung von castalagin, vescalagin, castalin and vescalin. *Justus Liebigs Ann. Chem.* **1967**, *707*, 177−181.
(26) Hervé du Penhoat, C.; Michon, V. M. F.; Ohassan, A.; Peng, S. Y.; Scalbert, A.; Gage, D. Roburin-A, a dimeric ellagitannin from heartwood of *Quercus robur*. *Phytochemistry* **1991**, *30*, 329−332.
(27) Hervé du Penhoat, C.; Michon, V.; Peng, S. Y.; Viriot, C.; Scalbert, A.; Gage, D. Structural elucidation of new dimeric ellagitannins from *Quercus robur* L. roburins A−E. *J. Chem. Soc., Perkin Trans. 1* **1991**, *1*, 1653−1660.
(28) Vivas, N.; Glories, Y. Role of oak wood ellagitannins in the oxidation process of red wines during aging. *Am. J. Enol. Vitic.* **1996**, *47*, 103−107.
(29) Del Álamo Sanza, M.; Nevares Domínguez, I. Wine aging in bottle from artificial systems (staves and chips) and oak woods: anthocyanin composition. *Anal. Chim. Acta* **2006**, *563*, 255−263.
(30) Del Álamo-Sanza, M.; Fernández-Escudero, J. A.; De Castro-Torío, R. Changes in phenolic compounds and colour parameters of red wine aged with oak chips and in oak barrels. *Food Sci. Techol. Int.* **2004**, *10*, 233−241.
(31) Jourdes, M.; Lefeuvre, D.; Quideau, S. *C*-Glycosidic ellagitannins and their influence on wine chemistry. In *Chemistry and Biology of Ellagitannins. An Underestimated Class of Bioactive Plant Polyphenols*; Quideau, S., Ed.; World Scientific Publishing: Singapore, 2009; pp 320−365.
(32) Quideau, S.; Jourdes, M.; Saucier, C.; Glories, Y.; Pardon, P.; Baudry, C. DNA topoisomerase inhibitor acutissimin A and other flavano-ellagitannins in red wine. *Angew. Chem., Int. Ed.* **2003**, *42*, 6012−6014.
(33) Brouillard, R.; Dubois, J. E. Mechanism of the structural transformations of anthocyanins in acidic media. *J. Am. Chem. Soc.* **1977**, *99*, 1359−1367.
(34) Brouillard, R.; Delaporte, B. Chemistry of anthocyanin pigments. 2. Kinetic and thermodynamic study of proton transfer, hydration, and tautomeric reactions of malvidin 3-glucoside. *J. Am. Chem. Soc.* **1977**, *99*, 8461−8468.
(35) Brouillard, R.; Lang, J. The hemiacetal-cis-chalcone equilibrium of malvin, a natural anthocyanin. *Can. J. Chem.* **1990**, *68*, 747−754.
(36) Pina, F.; Melo, M. J.; Laia, C. A. T.; Parola, A. J.; Lima, J. C. Chemistry and applications of flavylium compounds: a handful of colours. *Chem. Soc. Rev.* **2012**, *41*, 869−908.
(37) Pina, F.; Petrov, V.; Laia, C. A. T. Photochromism of flavylium systems. An overview of a versatile multistate system. *Dyes Pigments* **2012**, *92*, 877−889.
(38) Mora-Soumille, N.; Al Bittar, S.; Rosa, M.; Dangles, O. Analogs of anthocyanins with a 3,4-dihydroxy substitution: synthesis and investigation of their acid−base, hydration, metal binding and hydrogen-donating properties in aqueous solution. *Dyes Pigments* **2013**, *96*, 7−15.
(39) Pina, F.; Melo, M. J.; Parola, A. J.; Maestri, M.; Balzani, V. pH-controlled photochromism of hydroxyflavylium ions. *Chem.−Eur. J.* **1998**, *4*, 2001−2007.
(40) Nave, F.; Petrov, V.; Pina, F.; Teixeira, N.; Mateus, N.; de Freitas, V. Thermodynamic and kinetic properties of a red wine pigment: catechin-(4,8)-malvidin-3-*O*-glucoside. *J. Phys. Chem. B* **2010**, *114*, 13487−13496.
(41) García-Estévez, I.; Jacquet, R.; Alcalde-Eon, C.; Rivas-Gonzalo, J. C.; Escribano-Bailón, M. T.; Quideau, S. Hemisynthesis, structural and chromatic characterisation of myrtillin-vescalagin hybrid pigments. *J. Agric. Food Chem.* **2013**, DOI: jf4033188.
(42) Küster, F. W.; Thiel, A. *Tabelle per le Analisi Chimiche e Chimico-Fisiche*, 12th ed.; Hoepli: Milano, Italy, 1982.
(43) Leydet, Y.; Gavara, R.; Petrov, V.; Diniz, A. M.; Parola, A. J.; Lima, J. C.; Pina, F. The effect of self-aggregation on the determination of the kinetic and thermodynamic constants of the network of chemical reactions in 3-glucoside anthocyanins. *Phytochemistry* **2012**, *83*, 125−135.
(44) McClelland, R. A.; Gedge, S. Hydration of the flavylium ion. *J. Am. Chem. Soc.* **1980**, *102*, 5838−5848.
(45) Pina, F. Thermodynamics and kinetics of flavylium salts − malvin revisited. *J. Chem. Soc., Faraday Trans.* **1998**, *94*, 2109−2116. Correction in Scheme 1, see: Pina, F. *J. Chem. Soc., Faraday Trans.* **1998**, *94*, 3781.
(46) Jurd, L.; Geissman, T. A. Anthocyanins and related compounds. I. Structural transformations of flavylium salts in acidic solutions. *J. Org. Chem.* **1963**, *28*, 987−991.